J Appl Electrochem (2008) 38:189–195
DOI 10.1007/s10800-007-9422-1

ORIGINAL PAPER

All-solid secondary polyaniline-zinc battery

**P. Sivaraman · A. P. Thakur · R. K. Kushwaha ·
D. Ratna · A. B. Samui**

Received: 27 October 2006 / Revised: 9 September 2007 / Accepted: 12 September 2007 / Published online: 2 October 2007

Abstract A solid state battery based on polyaniline (PANI), Zinc (Zn) and a gel polymer electrolyte (GPE) is reported for the first time. Poly (ethylene oxide)–zinc sulphate-nanoclay-H_2O based GPE was used as the separator. The GPEs with a varying composition of salt were evaluated for their electrochemical performance. The highest conductivity at ambient temperature for the GPEs was found to be 5.54×10^{-4} S cm^{-1}. Cyclic voltammetry and impedance studies, with the Zn/GPE/Zn cell, showed reversibility with respect to Zn/Zn^{2+} couple. The battery showed a capacity of 43.9 Ah kg^{-1} of PANI and a coulombic efficiency higher than 100%. However, a decrease in capacity was observed for the system during the cycling.

Keywords Battery · Polyaniline · Gel polymer electrolyte · Zinc

1 Introduction

Over the last few decades there have been extensive research activities in conducting polymers because of their potential applications in various fields such as batteries, supercapacitors, chemical sensors, electrochromic display, electric devices etc. [1]. Among the various conducting polymers, polyaniline (PANI) has been the most widely studied due to the ease of synthesis, controllable electrical conductivity and an excellent environmental stability. These properties of PANI have prompted researchers to use it in rechargeable batteries. Compared to conventional secondary batteries, batteries made from conducting polymers offer several advantages such as high energy density, high voltage, low density and shape multiplicity. Moreover, conducting polymer-based electrodes are neither soluble nor do they undergo passivation during oxidation. Furthermore, there is no precipitation during charging/discharging. Hence, conducting polymers are excellent candidates for use as electrodes in battery applications. Zinc (Zn) based batteries have several advantages. Zn is very stable, has low toxicity [2] and can be easily handled even in the presence of moisture.

Poly (ethylene oxide) (PEO) based solid polymer electrolytes are very common in polymer batteries [1, 3]. It is well known that the amorphous region in PEO is responsible for the ionic conduction. The addition of inert fillers like ceramic nanoparticles to increase the amorphous phase of the PEO has been reported [4–7]. Scrosati [4] reported that the addition of inert fillers to the electrolytes increased the conductivity. PEO-based electrolytes have been utilized in solid state zinc batteries [8, 9]. Fauvarque et al. used a PEO–KOH based electrolyte in a solid state zinc–nickel battery [8]. Hagan et al. used a solid polymer electrolyte (PEO_n–ZnX_2) in a zinc battery [9].

Work on PANI-Zn batteries has mostly been based on liquid electrolytes [10–18]. However, no report is available in the literature on the use of solid electrolytes in PANI-Zn batteries. In this study we have used PEO–$ZnSO_4$-nanoclay-H_2O as the solid electrolyte and the separator in a PANI-Zn battery. A detailed study of gel polymer electrolytes (GPEs) for the application in PANI-Zn batteries is reported.

P. Sivaraman · A. P. Thakur · R. K. Kushwaha · D. Ratna ·
A. B. Samui (✉)
Naval Materials Research Laboratory, (DRDO),
Anand Nagar (PO), Ambernath, Maharashtra 421 506, India
e-mail: absamui@rediffmail.com

2 Experimental

2.1 Materials

PEO of molecular weight 6×10^5 g mol^{-1} was used in the preparation of GPE and was procured from Aldrich. The Teflon suspension (10% in ammonia) was received from Hindustan Fluoro Carbon Corp (India). Both were used without further purification. The organically modified clay was supplied by Nanocor Inc, IL, USA under the trade name of Nanomer. The conducting carbon powder (Vulcan XC-72) was received from Cabot Corporation (Japan). It was purified by soxhletting with water. The conducting carbon paper, from Toray, Japan, was used as received and the Zn metal used was of battery grade.

2.2 Preparation of gel polymer electrolyte

Organically modified clay was added to distilled water and sonicated in an ultrasonic bath for 15 min. $ZnSO_4$ was added to the mixture and stirred for 10 min followed by the addition of PEO. During the initial stage of mixing, the mechanical stirring was kept at slow speed for about 1 h. Mixing was continued under vigorous stirring for 4 h. The viscous solution was cast in a Teflon mould, dried in air for 24 h, and then dried in an air-circulating oven at 50 °C to constant weight. The composition of the PEO/$ZnSO_4$/nanoclay gel electrolyte was 10/X/0.75 (weight ratio). Three electrolyte compositions were prepared with X = 3, 4, 5 and coded as GPE1, GPE2 and GPE3 respectively. The amount of water in the polymer electrolyte was approximately 12–15% by weight.

2.3 Preparation of composite PANI electrode

PANI was synthesized chemically following the method of MacDiarmid et al [19]. Dedoping of PANI was carried out by stirring it in 0.5 M NH_4OH for 5 h. The dedoped PANI was filtered, washed with distilled water and dried at 50 °C for 48 h. PANI was purified by soxhletting with acetone for an extended period for complete removal of the low molecular weight fractions. The resultant powder was dried at 80 °C for 24 h and used for electrode preparation.

PANI powder was mixed with purified conducting carbon, Teflon suspension and the GPE solution. A 10% aqueous solution of GPE was used for electrode preparation. The requisite amount of polyacrylic acid was added to GPE solution so that the dry electrode formed maintained a pH value of 4.5. The composition of the PANI composite electrode is given in Table 1. The ratio of PANI/GPE/conducting carbon was maintained at 1/1/1 (by weight). The amount of Teflon was less than 0.05 wt.% of PANI, while the loading of PANI was 3.55 mg cm^{-2}. Three electrodes, with three different GPEs, were made as given in Table 1. The ingredients were mixed thoroughly to yield a paste. The paste was then applied to a carbon paper by the rolling method. After fabrication, the electrodes were kept in an oven with air circulation at 50 °C for 72 h.

Table 1 Composition of gel polymer electrolytes and PANI composite electrode

Sample	Composition (weight ratio)
Gel polymer electrolyte	
GPE1	PEO/$ZnSO_4$/nanoclay: 10/3/0.75
GPE2	PEO/$ZnSO_4$/nanoclay: 10/4/0.75
GPE3	PEO/$ZnSO_4$/nanoclay: 10/5/0.75
PANI composite electrode	PANI/Conducting carbon/GPE: 1/1/1

2.4 Cell construction

Symmetric cells SS/GPE/SS and Zn/GPE/Zn were assembled and sealed using plastic-coated aluminum foil. The PANI-Zn cell configuration was Zn/GPE/PANI. The charging/discharging studies of the PANI-Zn battery were carried out with a cell of size 2.5 cm × 2.5 cm.

2.5 Characterisation

Impedance analysis, cyclic voltammetry and charging/discharging analysis were carried out using an AUTOLAB (PGSTAT30) from Eco Chemie. The impedance analysis was carried out in the frequency range 100 kHz–0.01 Hz, and the area of the cells used was 1.5 cm^2. The amplitude of the ac voltage was 5 mV and all the experiments were carried out at ambient temperature.

3 Results and discussion

3.1 Characterization of solid polymer electrolyte

In our previous study the PEO/$LiClO_4$/nanoclay electrolyte was found to have maximum conductivity at a PEO/nanoclay weight ratio of 10/0.75 [20]. Hence, in the present study, the same ratio was used. GPEs with a varying concentration of salt in the polymer electrolyte were analyzed by impedance spectroscopy. The thickness of the GPE film was in the range 0.4–0.5 mm. Electrochemical impedance of the GPEs was studied using a SS/GPE/SS cell. Impedance plots for the three GPEs are shown in Fig. 1A. The absence of a semicircle suggests the existence

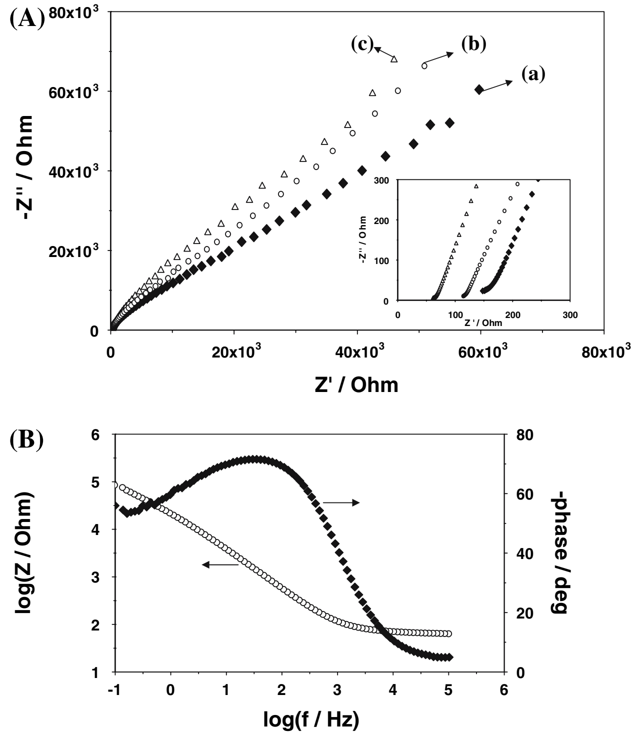

Fig. 1 (**A**) Impedance of PEO- $ZnSO_4$- nanoclay-H_2O gel polymer electrolyte (a) GPE1, (b) GPE2 and (c) GPE3. Inset shows the impedance at high frequency. (**B**) Bode plot for GPE3

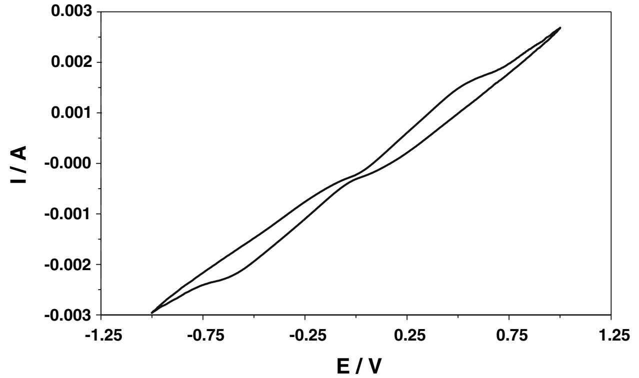

Fig. 2 Cyclic voltammogram of the Zn/GPE/Zn cell. Scan rate is 5 mV s^{-1}

of high resistance associated with the SS/GPE interface. This represents a resistor with a capacitor. The capacitive component becomes negligible at high ac frequency. The Bode plot for GPE3 is shown in Fig. 1B where the phase angle reaches a value close to 80°, indicating capacitive behaviour of the SS/GPE interface. The intercept on the real axis gives the resistance of the GPE. The specific conductance calculated for GPE1, GPE2 and GPE3 are 2.23×10^{-4}, 3.03×10^{-4} and 5.54×10^{-4} S cm^{-1} respectively, indicating that the conductivity of the GPE3 is the highest. The conductivity of PEO based polymer electrolytes depends on the ion type, ion concentration, $(O{:}M^+)$ ratio, temperature and pressure [21]. As the salt concentration increases in the GPE, the number of dissociated ions increases resulting in an enhancement of conductivity. The solvating power, as well as the flexibility of PEO chains, increase due to the addition of nanoparticles and results in increased conductivity of the polymer electrolyte. A similar observation was reported earlier [22, 23].

An increase in the salt concentration above x = 6, in the polymer electrolyte results in non-uniform film. Moreover, increasing the salt concentration results in the formation of ion pair $[M_2X]^+$ $[MX_2]^-$ and the ions are large in size with restricted mobility. Also, the aggregation of ions forms physical cross linking along the linear PEO chains, which decrease the flexibility and limit the ion mobility. Hence, the increase in conductivity may not be proportional to ion concentration above a critical concentration [21].

Figure 2 shows the voltammogram of the Zn/GPE/Zn cell obtained at a scan rate of 5 mV s^{-1}. The anodic and cathodic currents are symmetrical and the ratio of the cathodic to the anodic charge is 1.02. The plot illustrates the plating and stripping process and the reversibility of the Zn/Zn^{2+} couple. This result suggests that the PEO–$ZnSO_4$-nanoclay-H_2O electrolyte can be used for battery application with Zn as the anode. The cross potential is at 0 V. The anodic and cathodic peaks are separated by 1 V, a value much higher than that expected for a two electron-transfer reaction. In the Zn/GPE/Zn cell, one Zn electrode acts as the working electrode and the other as both the reference and counter electrodes. This leads to polarization of both the electrodes simultaneously, and hence a large difference in the peak potentials is observed. Moreover, the ohmic drop due to the GPE also adds to the high value observed [24].

The presence of an elongated semicircle in the impedance plot of the Zn/GPE/Zn cell (Fig. 3a) suggests that the Zn metal attains equilibrium with Zn ions present in the GPE. The high frequency impedance value is found to be 52 Ω, whereas the value at low frequency is 4×10^3 Ω. The high frequency impedance values are almost equal, whereas the low frequency values are much lower than that of a SS/GPE/SS cell. The low impedance value at the Zn/GPE interface can be attributed to the electrochemical activity of Zn. The extended semicircle suggests overlapping of two semicircles. This can also be explained on the basis of solid electrolyte interface (SEI) film formation [25, 26]. It is proposed that SEI film consists of a thin passivating layer towards the metal side (L_1) and a porous secondary layer of corrosion product over the passive layer (L_2). The L_1 film resistance R_f and its capacitance C_f can form a semicircle in the high frequency region. The semicircle at the low frequency end may be due to electrochemical equilibrium between the Zn and Zn^{2+} ions of

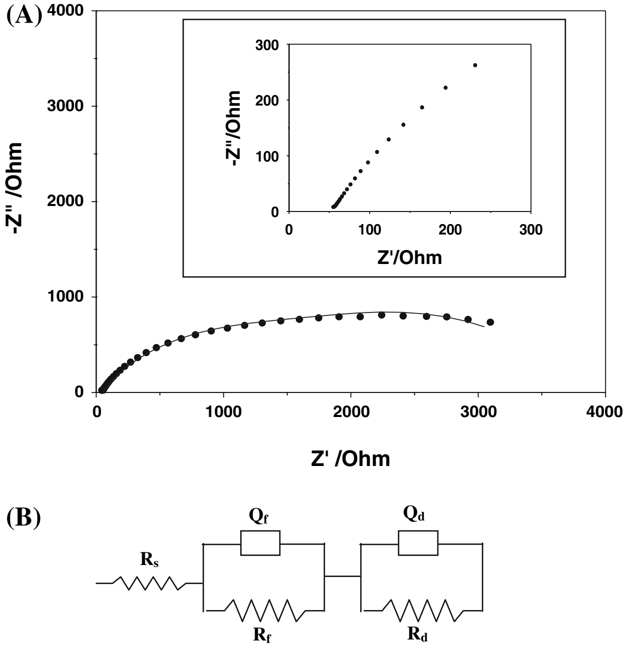

Fig. 3 (**a**) The impedance plot of Zn/GPE/Zn cell for GPE3. Inset shows the impedance at high frequency. The symbol shows the experimental data and solid line shows the simulate data (**b**) Equivalent circuit of the plot

the L_1 layer. The ions in the L_1 layer are in equilibrium with Zn^{2+} ions present in GPE. The Zn/GPE interface can be represented by an equilibrium circuit as shown in Fig. 3b. The solution resistance of the GPE is represented by R_s, the surface film resistance by R_f, the charge transfer resistance involving the Zn/Zn^{2+} couple by R_{ct} and the constant phase elements are represented by Q_f and Q_d. Since the semicircles are not perfect, the surface capacitance C_f and double layer capacitance C_d can be replaced with Q_f and Q_d respectively. The simulated curve is shown by the solid line in Fig. 3a. The simulated values are $R_s = 51.9\ \Omega$, $R_f = 2.77\ k\Omega$, $Q_f = 0.179 \times 10^{-6}\ \Omega^{-1}$, $n = 0.63$, $R_{ct} = 1.089\ k\Omega$, $Q_d = 0.181 \times 10^{-6}\ \Omega^{-1}$, and $n = 0.74$.

The Butler-Volmer equation is considered to be valid in a solid polymer electrolyte medium [26]. When an ac signal of very small amplitude is used, the Bulter-volmer equation can be simplified as

$$i_0 = \frac{RT}{2FR_{ct}} \tag{1}$$

where R_{ct} $\left(= -\frac{d\eta}{di}\right)$ is the charge transfer resistance. For a charge transfer resistance of $1.634 \times 10^3\ \Omega\ cm^2$, the exchange current density for the reaction $Zn \leftrightarrow Zn^{2+} + 2e^-$ is calculated as 7.91 $\mu A\ cm^{-2}$.

Transport number measurement was performed using a potentiostatic polarization technique in a cell of Zn/GPE/Zn configuration. A constant voltage of 20 mV was applied. The resultant current was monitored as a function of time [27]. The transport number for the Zn^{2+} ion can be calculated as the ratio of the initial current to the steady state current. Since the mobile cations in the GPE are complex ions such as triple and/or quadruple ions, t_+ does not strictly represent the transport number of Zn^{2+} ions. It is more accurately described as the dc conductivity, which transports Zn^{2+} ions from the negative to the positive electrode. The cation transference number for the GPE3 is 0.48. The addition of the nanoparticles to PEO based electrolytes has a pronounced effect on the value of the transference number. It has been shown that the cation transference number for PEO–lithium salt nanocomposite polymer electrolyte increased from 0.2–0.3 to 0.5–0.6 upon addition of the nanoparticles [27].

3.2 Characterization of PANI

Figure 4 shows the cyclic voltammogram of a PANI electrode at different scan rates. A three electrode configuration with PANI as the working electrode, platinum metal mesh as the counter electrode and Ag/Ag^+ as the reference electrode, was used for the characterisation. The PANI electrode composition was the same as that used in the battery configuration except for the solid electrolyte as the study was designed to be carried out in aqueous medium. The scan was carried out in an aqueous electrolytic solution of 1 M $ZnSO_4$ at pH 4.5. The cyclic voltammogram shows that PANI can well be doped electrochemically by sulphate dopants in the range from –0.3 to 0.8 V (Ag/Ag^+). The oxidation and reduction of PANI involves the insertion and deinsertion of sulphate dopants from the polymer. As expected, when the scan rate is increased, the oxidation peaks shift to higher, and the reduction peaks shift to lower, potentials, respectively. At 5 mV s^{-1}, the oxidation peak occurs at 0.125 V and the corresponding reduction peak occurs at 0.037 V (vs. Ag/Ag^+).

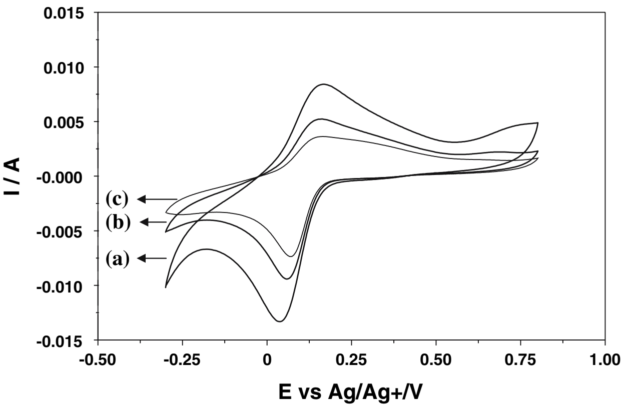

Fig. 4 Cyclic voltammogram of PANI electrode in 1 M $ZnSO_4$ aqueous solution at pH ~ 4.5. (a) 25 (b) 10 and (c) 5 mV s^{-1}

Electrochemically, PANI undergoes intrinsic redox processes.

3.3 Charging and discharging of PANI-Zn battery

It has been reported that PANI loses its electrochemical activity in solutions of pH > 4 [10]. On the other hand, Zn undergoes spontaneous dissolution in acidic media. This deficiency was overcome by constructing the PANI-Zn solid polymer battery in such a way that the PANI electrode was maintained in acidic pH while the Zn electrode was in neutral medium.

The cell configuration was Zn/GPE/(PANI + GPE). The Zn (anode) and the PANI (cathode) were separated by a 0.5 mm thick film of GPE3. In order to study the charge/discharge characteristics of individual electrodes, a silver wire was embedded inside the solid electrolyte as a quasi reference electrode. The open circuit potential of the cell was 1.2 V. At this potential, the PANI electrode was at 0.126 V (vs. silver wire) whereas the Zn electrode was at –1.074 V (vs. silver wire). From Fig. 4 it can be inferred that initially PANI is in the doped state. The doping of PANI takes place during the initial electrode fabrication process itself, via sulphate ions present in the GPE. Figure 5 illustrates the voltage profile of the cell, the PANI electrode and the Zn electrode respectively. When the cell is charged from 0.85 to 1.5 V, the PANI electrode is charged from –0.068 to 0.316 V (vs. silver wire) while the Zn electrode is charged from –0.923 to –1.195 V (vs. silver wire). During the discharge, the reverse of this process occurs.

In this study, all three compositions of the solid electrolyte were used in cell fabrication and were tested for their charge/discharge characteristics (Fig. 6). Galvanostatic charging/discharging was carried out at 1 mA. The discharge capacities of the battery with GPE1, GPE2 and GPE3 are 12.3, 18.4 and 43.9 Ah kg^{-1} respectively. The respective specific energy densities of the three GPEs are 14.8, 22.1 and 52.6 Wh kg^{-1}. Due to its good conductivity, the battery with GPE3 displays higher capacity compared to the other two.

The coulombic efficiency, observed for all the batteries, was above 100%. The cell with GPE3 was charged and discharged at 2 mA, 1 mA and 0.5 mA. The corresponding coulombic efficiencies were 103, 117 and 156% respectively. The higher coulombic efficiency may be due to the presence of oxygen in the system. It has been reported that PANI is easily oxidized (charged) by atmospheric oxygen [10]. The catalytic activity of PANI towards oxygen reduction in batteries has been reported earlier [28]. In the present system, a similar type of reaction may enhance the coulombic efficiency. Kitani et al and Shaolin et al reported coulombic efficiencies of 103% and 105% respectively [10, 12]. Saraswathi et al. reported a coulombic efficiency of approximately 150% for a Zn/sulphonated poly (*n*-methylaniline) battery [15].

A direct comparison cannot be made between the solid electrolyte based PANI-Zn battery studied in the present work and the aqueous electrolyte based PANI-Zn battery. Some of the reported values of energy density using aqueous electrolytes are in the range 20.7–146.4 Ah kg^{-1} [10–15].

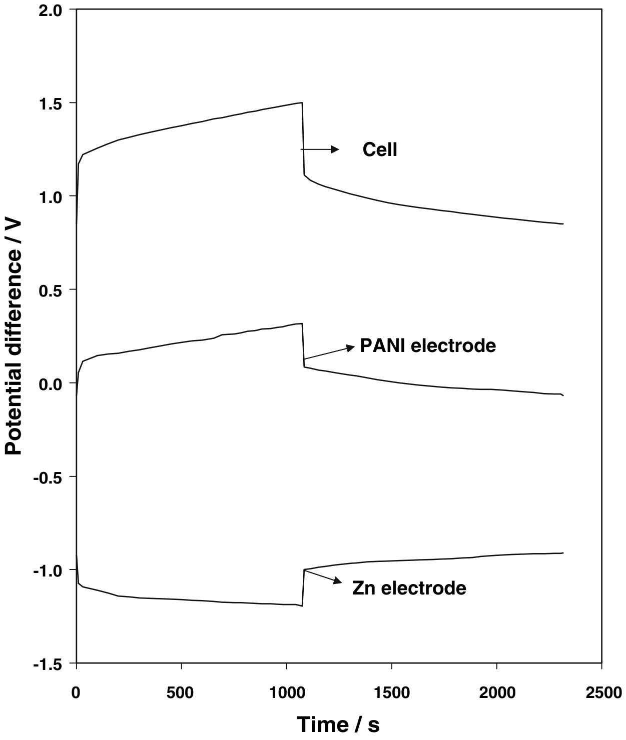

Fig. 5 Typical voltage profile of cell, PANI electrode and Zn electrode during charging and discharging

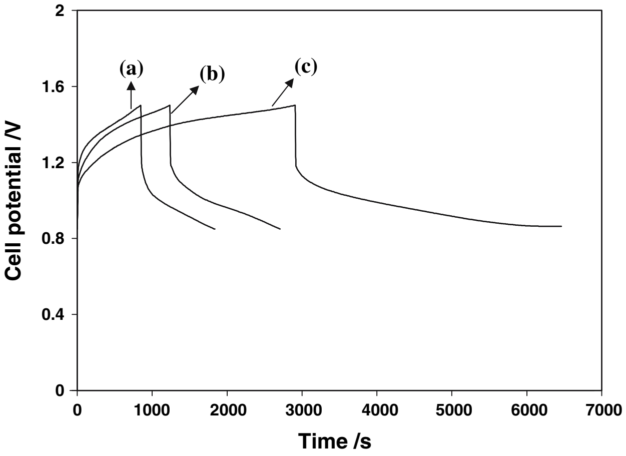

Fig. 6 Charge/discharge of PANI-Zinc battery of three GPE compositions. (a) GPE1 (b) GPE2 and (c) GPE3

It can be seen in Fig. 5 that during the discharge of the cell from 1.5 to 0.85 V, the PANI electrode sweeps between 0.314 and –0.068 V vs. silver wire. The time for discharge may be calculated from the discharge curve of the battery with GPE3 to be 3543 s (Fig. 6c). From this, the capacitance of the PANI electrode can be calculated as approximately 475 F g^{-1} of PANI. This value is quite high for PANI with a gel polymer electrolyte. However, the value should be taken with caution because the capacitance is known to depend on the discharge rate [29]. A value of 350 F g^{-1} of PANI with GPE was reported by Munichandraiah et al [30].

3.4 Cycling studies

The battery with GPE3 was further subjected to charge/discharge cycles. It is reported that the upper and lower cut off voltage during charge/discharge affects the coulombic efficiency of the PANI-Zn batteries [10, 11]. Hence in the present case, the galvanostatic charge/discharge study was carried out in the range 0.9 to 1.35 V at 1 mA (Fig. 7) for 40 cycles. Beyond 40 cycles, the capacity decreases sharply (not shown). The coulombic efficiency of the battery is above 100%. It decreases sharply from 178% during the initial 10 cycles and attains a constant value around 105%. The capacity of PANI-Zn solid electrolyte battery increases from 14.1 Ah kg^{-1} to reach the maximum value of 16.1 Ah kg^{-1} at the 10th cycle and then decreases to 11.2 Ah kg^{-1} of PANI at the 40th cycle. During the initial cycling, there might be a decrease in the resistance of the composite PANI electrode and the gel polymer electrolyte due to the formation of a path for the easy diffusion of ions. This, in turn, might increase the capacity of the battery initially. However the decrease in capacity during later cycling can be attributed to the degradation of the Zn/electrolyte interface. Also, the sulphate ions present in the system degrade PANI during prolonged cycling [30]. Rahmanifar [17] showed that the formation of a new material on the Zn electrode acts as the passive layer, and this reduces the cycling efficiency of the battery. In lithium polymer batteries, it has been reported that the decrease in capacity was generally due to degradation of the Lithium/electrolyte interface during the plating and stripping cycle. In the present study, this kind of layer formation increases the resistivity of the solid electrolyte which, in turn, increases the IR drop of the cell during cycling.

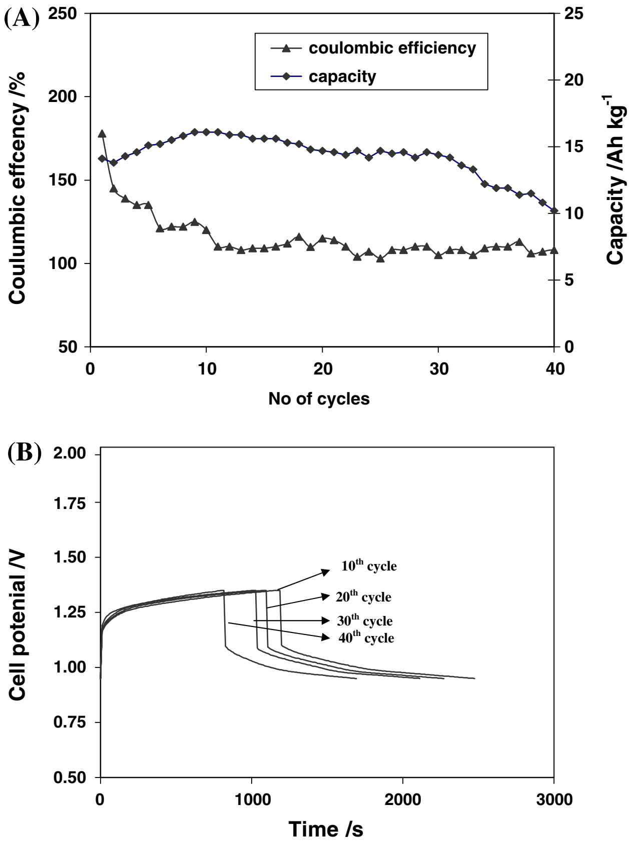

Fig. 7 (**a**) Columbic efficiency and capacity of the PANI-Zinc solid battery (**b**) Charge–discharge cycle at different cycles

4 Conclusion

A gel polymer electrolyte based on PEO–$ZnSO_4$-nanoclay was prepared and characterized for use in a solid PANI-Zn battery. The conductivity of the gel polymer was measured by varying the PEO/$ZnSO_4$ ratio and it was observed that the gel electrolyte with PEO/$ZnSO_4$/nanoclay ratio of 10/5/0.75 (GPE3) exhibited the highest conductivity. The impedance and cyclic voltammetry studies of the gel polymer electrolyte showed the reversible nature of the Zn/Zn^{2+} couple. The Zn/GPE interface was analyzed by an equivalent circuit diagram. The battery with GPE3 has shown a capacity of 43.9 Ah kg^{-1} of PANI and a specific energy density of 52.6 Wh kg^{-1}. The cycling study indicated that the capacity tends to fade during cycling. The battery showed a coulombic efficiency higher than 100%.

Acknowledgement The authors thank Dr. J. Narayana Das Director, NMRL for his encouragement and permission to publish this work.

References

1. Malhotra BD (2002) Handbook of polymers in electronics. Rapra Technology Ltd., UK
2. Linden D (1984) Handbook of batteries. McGraw-Hill, New York
3. Scrosati B (1993) Applications of electroactive polymers. Chapman & Hall, London
4. Scrosati B, Croce F, Persi L (2000) J Electrochem Soc 147:1718

5. Croce F, Persi L, Ronci F, Scrosati B (2000) Solid State Ionics 47:315
6. Lemmon JP, Wu J, Oriakhi C, Lerner MM (1995) Electrochim Acta 40:2245
7. Wiecrorek W, Florjanczyk Z, Stevens JR (1995) Electrochim Acta 40:2251
8. Fauvarque JF, Guinot S, Bousir N, Salmon E, Penneau JF (1995) Electrochim Acta 40:2449
9. Hagan WP, Latham RJ, Linford RG, Vickers SI (1994) Solid State Ionics 70/71:666
10. Kitani A, Kaya M, Sasaki K (1986) J Electrochem Soc 133:1069
11. Trinidad F, Montemayor MC, Fatas E (1991) J Electrochem Soc 138:3186
12. Shaolin M, Jinhai Y, Yuhua W (1993) J Power Sources 45:153
13. Rahmanifar MS, Mousavi MF, Shamsipur M (2002) J Power Sources 110:229
14. Sima M, Visan T, Buda M (1995) J Power sources 56:133
15. Siva Kumar R, Saraswathi R (2002) J Power Sources 104:226
16. Karami H, Mousavi MF, Shamsipur M (2003) J Power Sources 124:303
17. Rahmanifar MS, Mousavi MF, Shamsipur M, Ghaemi M (2004) J Power Sources 132:296
18. Karami H, Mousavi MF, Shamsipur M, Riahi S (2006) J Power Sources 154:298
19. MacDiarmid AG, Chiang JC, Richter AF, Epstein AJ (1987) Synth Met 18:393
20. Ratna D, Diwakar S, Sivaraman P, Samui AB, Chakraborty BC (2007) Polym Int 56:900
21. Robitaille CD Fauteux D (1986) J Electrochem Soc 133:315
22. Croce F, Persi L, Scrosati B, Serraino-Fiory F, Plichta E, Hendrickson MA (2001) Electrochem Solid State Lett 4:A121
23. Persi L, Croce F, Scrosati B, Plichta E, Hendrickson MA (2002) J Electrochem Soc 149:A212
24. Girish Kumar G, Sampath S (2003) J Electrochem Soc 150:A608
25. Girish Kumar G, Munichandraiah N (2000) Solid State Ionics 128:203
26. Munichandraiah N, Scanlon LG, Marsh RA, Kumar B, Sircar AK (1994) J Electroanal Chem 379:495
27. Chung SH, Wang Y, Persi L, Croce F, Greenbaum SG, Scrosati B, Plichta E (2001) J Power Sources 97–98:644
28. Barukov VZ, Khomenko VG, Chivikov SV, Barsukov IV, Montronyuk TI (2001) Electrochim Acta 46:4083
29. Conway BE (1999) Electrochemical supercapacitors, scientific fundamentals and technological application. Kluwer Academic/Plenum, New York
30. Rajendra Prasad K, Munichandraiah N (2002) Electrochem Solid State Lett 5:A271